

## Piezoquartz Resonator as an In Situ Method for Studying the Phase Transitions in Thin Metal and Alloy Films

M. M. Kolendovskii, S. I. Bogatyrenko, A. P. Kryshstal\*, and N. T. Gladkikh

Karazin Kharkiv National University, pl. Svobody 4, Kharkiv, 61077 Ukraine

\*e-mail: kryshstal@univer.kharkov.ua

Received June 15, 2011

**Abstract**—A new method based on a quartz resonator is proposed to study the melting–solidification phase transformations in metal and alloy nanofilms. The melting–solidification temperature hysteresis is studied, and the supercoolings upon the solidification of bismuth and gold–germanium films on a carbon substrate are determined. The results obtained by the new method are shown to agree well with the reported data.

**DOI:** 10.1134/S1063784212060175

### INTRODUCTION

The melting–solidification phase transformations have been extensively studied in free particles and thin films of many metals, which are usually deposited onto amorphous inert substrates [1, 2]. For binary systems, such data are rather scarce, especially for small sizes, which is caused by the fact that only in situ methods (i.e., the methods in which nano-objects are prepared and studied in one cycle) can give reliable information on nano-objects due to their extremely high sensitivity to various impurities. Naturally, every in situ technique imposes certain experimental restrictions. For example, when high-resolution transmission electron microscopy is used [3], it is difficult to determine the action of an electron beam on the effects to be studied. The measurement of the electrical resistance of film systems, in which a low-melting-point component film is placed between refractory films, can mainly be applied for polycrystalline materials with a good electrical conductivity [4, 5]. High-precision differential scanning nanocalorimetry is applicable for materials with a high thermal conductivity, i.e., as a rule for metals [6].

Therefore, it is necessary to search for a method that could be used to investigate the phase transitions in systems with any types of interaction between their components and any conduction. In this work, we propose to use a quartz resonator for these purposes; it represents an electromechanical system based on the forward and reverse piezoelectric effects. Quartz resonators have a high Q factor ( $10^4$ – $10^7$ ) and a high frequency stability ( $10^{-6}$  or higher), and they have a very weak hysteresis during mechanical, temperature, and electrical actions. Owing to these properties, quartz is widely used in reference frequency generators, temperature sensors, pressure sensors, force sensors, and so on [7].

Sauerbrey [8] proposed to use a quartz crystalline resonator to determine low amounts of a deposited substance and showed that a thin film deposited onto the surface of a quartz electrode decreases its resonance frequency in proportion to the film mass,

$$\Delta f = -\frac{2f_0^2}{\sqrt{\rho_q \mu_q}} \Delta m, \quad (1)$$

where  $\Delta m$  is the film mass per unit area of the electrode;  $\rho_q$  and  $\mu_q$  are the quartz density and shear modulus, respectively; and  $f_0$  is the resonance frequency.

This method is now widely used to control the mass thickness of condensed films accurate to several fractions of a nanometer. The basic condition of the applicability of the Sauerbrey equation is a rigid coupling between a condensate and the quartz plate surface; that is, it does not take into account the viscoelastic properties of a film. Later, it was shown that stable quartz vibrations can be obtained when quartz is in contact with a fluid, and the authors of [9] derived an expression that describes the change in the resonance frequency as a function of viscosity  $\eta_l$  and density  $\rho_l$  of the liquid in contact with quartz,

$$\Delta f = -f_0^{3/2} \sqrt{\frac{\rho_l \eta_l}{\pi \rho_q \mu_q}}. \quad (2)$$

Since the resonance frequency of quartz is sensitive to the mass thickness and viscosity of the film on its surface, its melting or solidification would change the resonance frequency of the quartz resonator because of a jumplike change in the viscosity. To date, a quartz resonator has been applied to study the phase transitions in polymer films upon heating [10, 11] and NaCl films during a change in the humidity [12].

The purpose of this work is to investigate the melting and solidification of thin metal and alloy films using a quartz resonator as a substrate. The jumplike

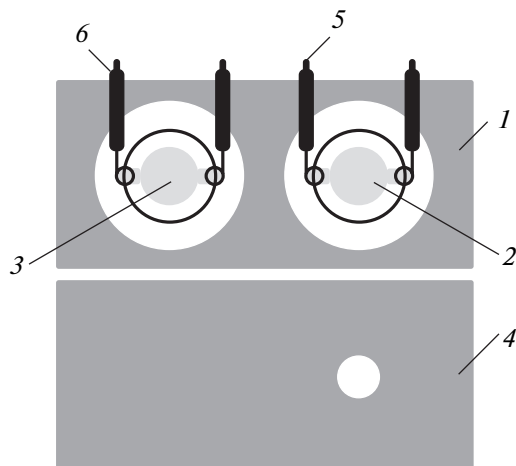


**Fig. 1.** Schematic diagram of the thermostat: (1) copper tank with a resistive heater, (2) quartz plate onto which a film system is condensed, (3) reference quartz plate, (4) copper mask closing quartz (shown separately), (5) contacts, and (6) insulators.

change in the resonance frequency and Q factor of the quartz resonator in heating and cooling is used to detect a change in the phase state of the film condensed on its surface.

## EXPERIMENTAL

The experiments were carried out as follows. Two identical quartz plates were placed in a copper thermostat equipped with a resistive heater, and a carbon film 20–30 nm thick was deposited onto one of them by vacuum arc evaporation through a mask (Fig. 1). Carbon was necessary to prevent an interaction between the film and the quartz resonator surface. Then, a film system to be studied was prepared by sequential condensation of components during thermal evaporation from independent sources at a rate of 2–3 nm/s. The experiments were performed in both a standard vacuum VUP-5M device equipped with a diffusion pump at a residual gas pressure of  $5 \times 10^{-5}$  Torr and a high-vacuum device with an oil-free pumping out system and a residual gas pressure of  $5 \times 10^{-8}$  Torr. The mass thickness of the condensed films was controlled from the shift in the resonance frequency of the quartz plate serving as a substrate. The second plate served as a temperature sensor, since it was impossible to measure the temperature of the quartz plate and the temperature dependence of its frequency was preliminarily calibrated against reference *K*-type thermocouples. The absolute accuracy of determining the quartz resonator temperature was 2°C, and the relative accuracy was 0.1°C. Heating and cooling were performed at a rate of 2–3°C/min in the temperature range 20–400°C. In some experiments, a miniature Pt resistor was fixed to the second quartz plate in order to increase the accuracy in the room temperature range,

and its resistance was used to determine the temperature in the thermostat.

For investigations, we used unpolished AT-cut quartz crystals with a fundamental harmonic resonance frequency of 4.608 MHz and a silver electrode  $\pm 6$  mm in diameter. The parameters of the quartz resonator upon heating and cooling were determined by the following two methods.

In the first method, a quartz plate was placed in the circuit of the positive feedback of a master oscillator, and a digital frequency counter was connected to its output to record the frequency of the sequential quartz resonance accurate to 1 Hz. The power dissipated in the crystal did not exceed 1 mW.

In the second method, a quartz resonator was connected to a characteristic tracer made of a digital oscilloscope and a swept frequency generator. The accuracy of determining the frequency was 3–5 Hz. The characteristic tracer made it possible to control both the frequency and Q factor of the quartz resonator, and the accuracy of determining this factor was about 5%.

All elements of the system of heating and measuring the quartz resonator parameters made up a program–apparatus complex that fully automated the processes of heating, cooling, and data acquisition.

After cooling to room temperature, the quartz resonator was removed to air and the film system on its surface was analyzed in a Jeol JSM-840 scanning electron microscope equipped with an EDS-1 electron-probe microanalysis attachment, which can detect elements beginning from boron.

We studied Al films 300 nm thick, Bi films 30 and 100 nm thick, and a layered Au/Ge film system 120 nm thick with the eutectic ratio of the components that were deposited onto an amorphous carbon substrate.

The choice of Al is caused by the necessity of studying the sensitivity of a quartz resonator to the relaxation and recrystallization processes that occur intensely in nonequilibrium polycrystalline Al films during low-temperature annealing.

The melting and solidification of Bi on a carbon substrate are well understood. There exist much data on the phase transitions in bismuth films and particles having various sizes and condensed under various vacuum conditions, and a comparison of these data with the results obtained with a quartz resonator will allow us to test the new method.

The components of the Au–Ge system form a eutectic phase diagram with a strongly limited solubility in the solid state and an infinite solubility in the liquid state [13] and with a eutectic melting temperature of 361°C, which is well below the melting temperatures of pure Au and Ge. At present, the phase transitions in binary systems are poorly understood (there is no generally accepted opinion regarding the mechanism and nature of eutectic melting); therefore, to obtain new data on the formation and temperature

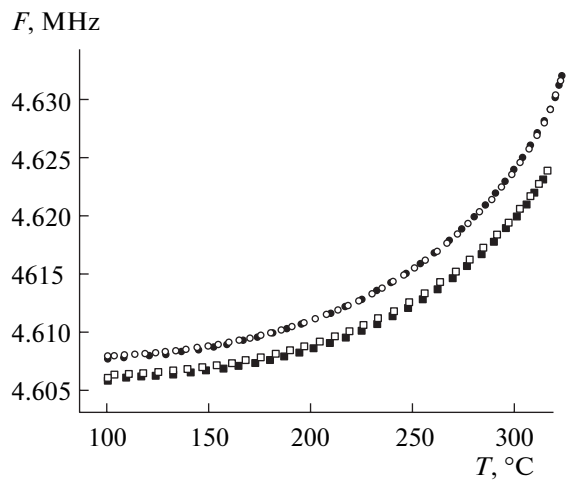


**Fig. 2.** Temperature dependences of the quartz plate frequency ( $\circ$ ●) before and ( $\blacksquare$ ) after deposition of an Al/C system. Solid points correspond to heating, and open points correspond to cooling.

stability of the liquid phase in such systems is a challenging problem.

## RESULTS AND DISCUSSION

### Al/C System

Figure 2 shows the dependence of the resonance frequency of the quartz resonator on its temperature in a heating–cooling cycle. It is seen that the resonance frequency of the AT-cut quartz resonator changes significantly beginning from a temperature of 80–100°C and that the sensitivity of quartz reaches 180 Hz/K at a temperature of 300°C. In this case, the temperature dependence of the resonance frequency is satisfactorily described by a third-degree polynomial, which agrees with the data in [7]. Note also that the  $F(T)$  curves recorded upon heating and cooling of a quartz plate coincide within a measurement point, which indicates the absence of temperature hysteresis and the reliability of determining the quartz resonator temperature.

Then, we sequentially deposited an amorphous carbon film 20–30 nm thick and a 300-nm-thick aluminum film onto a quartz plate at room temperature without breaking vacuum. The temperature dependence of the resonance frequency of the quartz resonator with an Al/C film system upon annealing to 320°C is shown in Fig. 2.

This dependence is also a monotonically increasing function shifted in frequency with respect to the corresponding dependence of pure quartz. The shift at room temperature corresponds to the mass thickness of deposited aluminum and increases smoothly with the temperature. The coincidence of the temperature dependences of the frequency in the Al/C system upon heating and cooling points to the fact that the

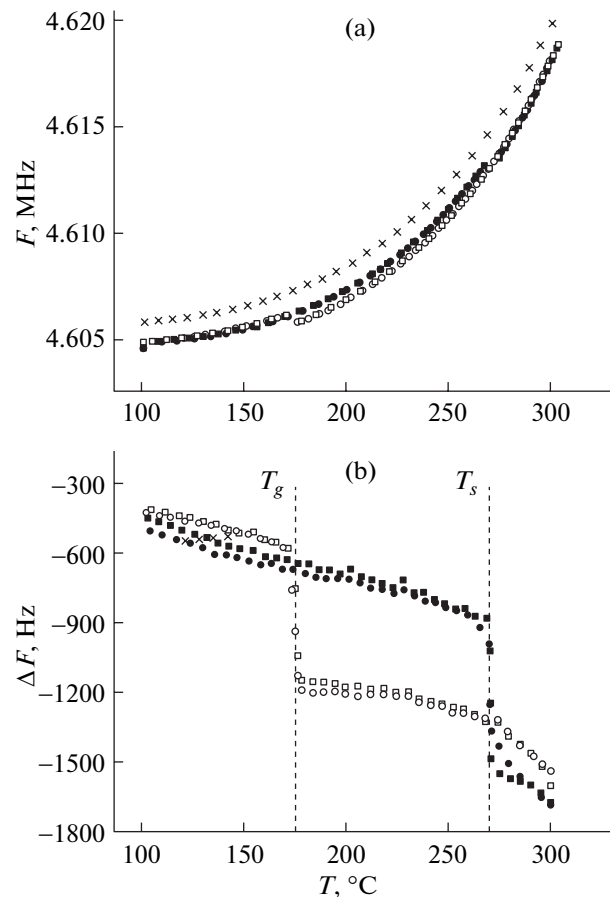


**Fig. 3.** Temperature dependences of the (a) frequency and (b) difference between the frequencies of pure quartz and quartz with a Bi film: ( $\blacksquare$ ) pure quartz and ( $\bullet$ ○) 1 and ( $\times$ ) 2 heating–cooling cycles for a 30-nm-thick bismuth film. Solid points correspond to heating, and open points correspond to cooling.

resonance frequency of the quartz resonator is insensitive to the processes that occur during low-temperature annealing of the films. Therefore, no difficulties with the interpretation of the experimental results should appear when the melting–solidification phase transitions in the condensed films are studied by the proposed method. In other words, a one-to-one correspondence can exist between the shift in the resonance frequency and the melting and solidification temperatures.

### Melting–Solidification of Bismuth Films

Bismuth films 30 nm thick were condensed in a vacuum of  $10^{-5}$  Torr onto a quartz plate coated with a preliminarily deposited carbon film and having room temperature. We then measured the resonance frequency in two heating–cooling cycles in the temperature range 100–300°C (Fig. 3a).

It is seen that the resonance frequency of quartz increases monotonically in heating, decreases jump-

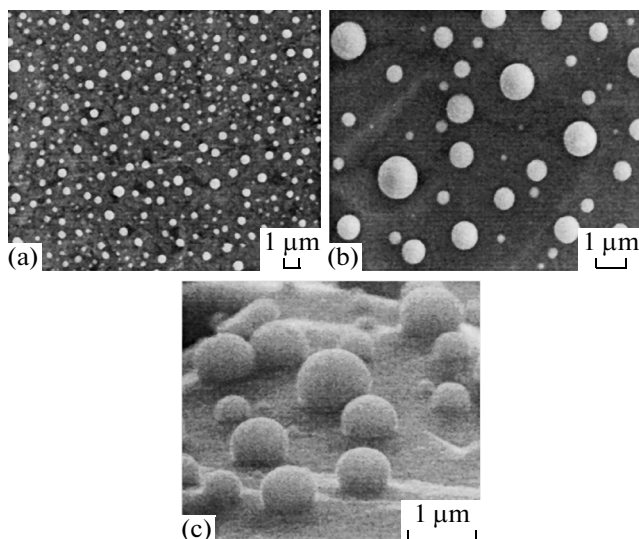


**Fig. 4.** Electron micrographs of a Bi/C system on a quartz plate with a bismuth mass thickness of (a) 30 and (b), (c) 100 nm after melting. (c) Image taken at an angle of  $75^\circ$  to the optical axis of the microscope.

wise at  $271^\circ\text{C}$ , and then increases monotonically. Upon cooling, the resonator frequency decreases monotonically, increases sharply at  $175^\circ\text{C}$ , and reaches the values obtained upon heating. For comparison, we also show the  $F(T)$  dependence of quartz before depositing a bismuth film (Fig. 3a).

This effect is most pronounced in Fig. 3b, which depicts the temperature dependence of the difference in the quartz frequencies before and after the deposition of a Bi film for two successive heating–cooling cycles. The temperature hysteresis that is related to a sharp change in the viscoelastic properties of the film system and corresponds to the melting ( $T_s$ ) and solidification ( $T_g$ ) of the Bi film is clearly visible.

Electron-microscopic examination of the quartz resonator surface after the heating–cooling cycles demonstrates that the Bi film consists of individual islands having the shape of a spherical segment (Fig. 4), which unambiguously indicates its melting [14, 15].

Note that there is no rigorous model describing the response of a quartz resonator to a change in the phase state of a thin film on its surface. The existing methods and approaches were reviewed in, e.g., [16]. As a rule, researchers consider the interaction of an ideally smooth quartz surface with a viscous Newtonian liquid. An oscillating quartz surface creates a plane-parallel laminar stream in the liquid, which causes the damping of the resonator and a decrease in its resonance frequency in proportion to  $(\rho_l\eta_l)^2$ . If the surface is rough (as in a real experiment), the interaction with the liquid becomes much more complex: new mechanisms, such as a turbulent flow and the capture of the liquid by surface cavities and pores, appear. As a result, the response of quartz begins to depend on many

parameters [16, 17]. Moreover, at a liquid layer thickness comparable with  $\delta = (\eta_l/\pi f \rho_l)^{1/2}$  (where  $\delta$  is the quantity reciprocal to the absorption coefficient and is determined as the distance along which the amplitude of a transverse (shear) sound wave decreases by  $e$  times), the resonance frequency depends on the film thickness nonmonotonically. In other words, films having different thicknesses cause the same change in the resonance frequency. In terms of this model, the changes in the resonance frequencies of quartz covered with solid and liquid films almost coincide at a film thickness  $t < \delta$  [12].

When analyzing the temperature dependences of the quartz resonator frequency obtained in two heating–cooling cycles, we note the following. The morphology of the bismuth films differs substantially before the beginning of the first and second cycles. The condensation of Bi onto an amorphous carbon substrate having room temperature occurs according to the Völmer–Weber mechanism, and the Bi film at a thickness of 30 nm is almost a continuous polycrystalline film [15]. Upon melting in the first cycle, it decomposes into islands with the maximum probable size larger than the initial film thickness by a factor of 12 [15, 18]. As is seen in Fig. 3, the changes in the frequency and the phase transition jump almost coincide in both cycles. Moreover, the quartz resonator frequencies at room temperature in the cases of continuous and island films also coincide. These findings point to the fact that the quartz resonator frequency for a polycrystalline film depends only on its mass thickness and is independent of its morphology. If we use the concepts developed in [12, 16], the coincidence of the frequencies of continuous and island films indicates the absence of friction between the quartz surface and islands. In other words, despite the insignificant contact between solidified drops and the surface (contact angle is  $\approx 120^\circ$ ), they are still rigidly coupled to it, at least at the quartz plate oscillation amplitudes used in this work.

The jump of the resonance frequency during the phase transition was found to depend on the bismuth film thickness. We failed to detect a change in the frequency in melting or solidification at Bi mass thicknesses  $h < 15$  nm, which is likely to be caused by the fact that the size of the particles forming upon melting of such a film becomes comparable with or smaller than  $\delta$  (which is  $\sim 100$  nm for Bi) and that the resonance frequency of quartz becomes almost insensitive to the phase state of the particles on the Bi surface [12]. When the film mass thickness decreases, the jump becomes comparable with the temperature-induced change in the quartz resonator frequency, which hinders its reliable detection. At  $h > 100$  nm, the oscillations of a quartz plate are significantly damped, which leads to the self-excitation of the generator and a break in generation.

Therefore, we used a characteristic tracer to record the quartz resonator parameters in our further investi-

gations, since it can record both the frequency and Q factor of the quartz resonator. The experiments were performed in an ultrahigh-vacuum device at a residual gas pressure of  $5 \times 10^{-8}$  Torr.

Figure 5 shows the temperature dependences of the Q factor of pure quartz and a quartz resonator with a 100-nm-thick Bi/C film system for the first three heating-cooling cycles. It is seen that, in contrast to the resonance frequency, the Q factor of pure quartz is almost temperature independent. Recall that the Q factor is determined as the ratio of the frequency to the peak width at  $1/\sqrt{2}$  amplitude and characterizes the energy losses in an oscillating system. When a liquid phase forms in the system, part of the quartz energy is consumed for oscillation film motion. Correspondingly, the Q factor of the resonator decreases sharply simultaneously with the frequency jump (Fig. 5) and returns to its initial value during film solidification. Moreover, the contact zone of a liquid drop with a quartz plate is insignificant; therefore, the effects related to drop sliding over the surface can appear and result in additional energy losses for friction.

Thus, our studies of the temperature dependence of the Q factor of the quartz resonator show that it is more sensitive and convenient for detecting phase transitions than the resonance frequency measurements.

The melting temperature in the Bi/C system determined at the point of the maximum rate of change of the Q factor is  $272^\circ\text{C}$ , and the solidification temperature of the supercooled liquid phase is  $118^\circ\text{C}$ . As in the previous experiment, the temperature dependence of the Q factor of the quartz resonator in the next heating-cooling cycles almost fully repeats its change in the first cycle.

It should be noted that solidification temperatures  $T_g$  obtained in two experiments on the Bi/C system are different at the same melting temperature of the system (Figs. 3, 5). These experiments differ substantially in the conditions of film system preparation. The solidification temperature is known to depend on both the character of interaction with a substrate and the presence of various impurities, including gas ones [12]. For example, the solidification temperature of Bi films deposited onto carbon substrates at the same condensation rate under different vacuum conditions varies from  $88$  to  $157^\circ\text{C}$ . It was shown that a significant change in the solidification temperature begins from a certain critical residual gas pressure and that a reliable determination of  $T_g$  requires experiments in a vacuum better than  $5 \times 10^{-8}$  Torr at a condensation rate of several nanometers per second. The values of  $T_g$  obtained in this work are  $118$  and  $175^\circ\text{C}$  at a residual gas pressure of  $5 \times 10^{-8}$  and  $10^{-5}$  Torr, respectively; these values are slightly higher than those obtained in [2] from a change in the vapor-crystal/vapor-liquid condensation mechanism. This difference is likely to be caused by different inflow and outflow wetting angles.

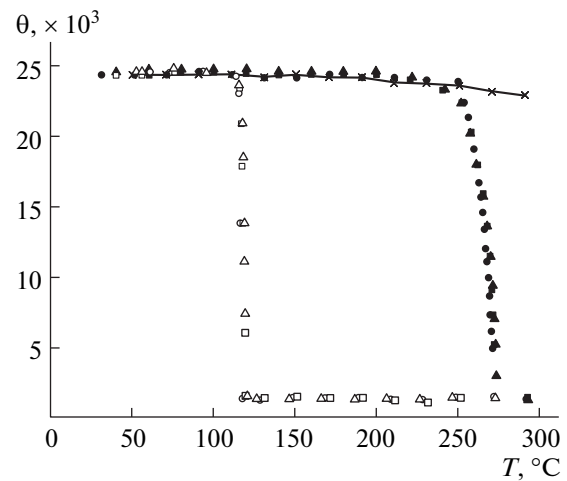
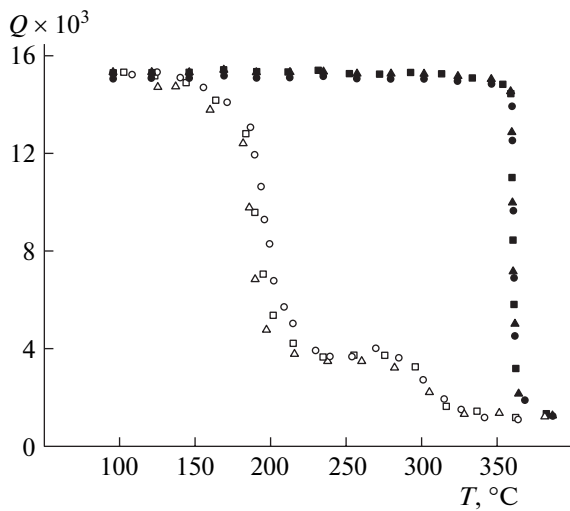


Fig. 5. Temperature dependence of the Q factor of a quartz resonator made of (×) pure quartz and quartz with a Bi film for (■□) 1, (●○) 2, and (×) 3 cycles. Solid points correspond to heating, and open points correspond to cooling.

For example, the angle of wetting a carbon substrate in the case of bismuth condensation into a supercooled liquid phase is  $\approx 130^\circ$  and is essentially determined by the wetting angle of a liquid nucleus forming at the initial stage of film growth. When a continuous film melts, islands form due to its decomposition and subsequent coalescence of droplets. In this case, the contact angle corresponds to the outflow wetting angle and turns out to be lower than the equilibrium value. Thus, the solidification temperature ( $118^\circ\text{C}$ ) determined under “pure” vacuum conditions with a quartz resonator and the measured wetting angle in the system ( $120^\circ$ ) correlate with the reported data for this system and the generalized dependence of the supercooling upon solidification on the degree of interaction with a substrate [2].

#### *Au-Ge Eutectic System*

A 40-nm-thick Ge film and a 80-nm-thick Au film were successively condensed in a vacuum of  $5 \times 10^{-8}$  Torr onto a quartz plate covered with a preliminarily deposited carbon film and having room temperature. The system was then heated to a temperature of about  $400^\circ\text{C}$ , and the corresponding changes in the quartz resonator parameters were recorded. Figure 6 shows the temperature dependences of the Q factor of the quartz resonator with the Au/Ge film system for the first three heating-cooling cycles. It is seen that all dependences exhibit a reproducible temperature hysteresis, which corresponds to the formation and solidification of a liquid phase in the system. The melting and solidification temperatures determined at the points with the maximum change of the Q factor are  $361$  and  $194^\circ\text{C}$ , respectively. Therefore, the supercooling during the solidification of the liquid phase in the Au/Ge system on a carbon substrate is  $165$  K.



**Fig. 6.** Temperature dependence of the Q factor of a quartz resonator with an Au/Ge film system. (■□) 1, (●○) 2, and (▲▲) 3 heating–cooling cycles. Solid points correspond to heating, and open points correspond to cooling.

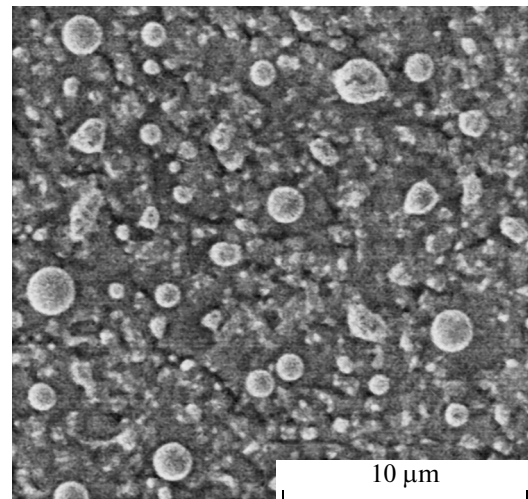


**Fig. 7.** Electron micrograph of an Au/Ge/C system on a quartz plate with a mass thickness of 120 nm after heating to 400°C.

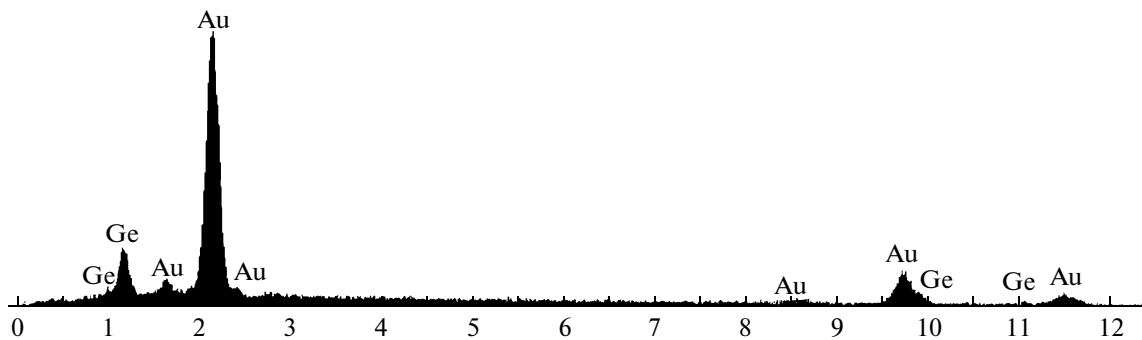


**Fig. 8.** X-ray spectrum of a spherical particle.

The mechanism of liquid phase formation represents a substantial difference of this system from the Bi/C system. At the initial time, a clear interface existed in the system, since the Au/Ge system was formed by successive condensation and the solubility of gold in germanium is very low. In heating, contact melting occurred in the film contact zone at 361°C and a liquid phase based on gold and germanium formed there. Since the ratio of the film mass thicknesses corresponded to the eutectic ratio, the quantity of the liquid phase increased (according to the phase diagram), which resulted in a break in the continuity of the film and its decomposition into islands. This nonuniform decomposition led to different ratios of the components in islands because of a high quartz surface roughness and a large film system thickness. In the islands where the ratio of the gold to the germanium mass was close to the eutectic ratio, almost the entire substance transformed into a liquid state and formed drops, since the liquid Ge–Au eutectic does

not wet a carbon sublayer. In the other islands, an excess component was retained as a solid phase based on it, according to the phase diagram.

This scenario is supported by the electron-microscopic studies of the morphology of the film system on the quartz resonator surface after cooling to room temperature (Fig. 7). Spherical and near-spherical particles consisting of the solidified eutectic, irregular islands with molten edges, and small eutectic particles ( $\sim 0.3 \mu\text{m}$ ) in contact with the germanium film are clearly visible.

A quantitative analysis of the composition of individual particles by X-ray spectroscopy supports the fact that the spherical particles have a near-eutectic composition and that the amount of an excess component (in this case, gold) increases as the particle shape degrades (Fig. 8). Integral analysis of the film system composition from a  $100 \times 100\text{-}\mu\text{m}$  area gives an almost eutectic ratio of the gold and germanium masses.

Upon cooling to the solidification temperature, the liquid phase decomposes into almost pure germanium and a gold-based solid solution, which results in a sharp change in the conditions of acoustic vibration propagation in the quartz resonator and, correspondingly, in a change in its Q factor (Fig. 6). In contrast to the one-component system, the liquid phase solidifies in the temperature range 150–210°C, which is explained by the dependence of the composition of the liquid phase in the binary system [2]. In all cycles, the Q factor changes insignificantly at a temperature of  $\approx 310^\circ\text{C}$ . This effect is assumed to be related to the fact that small eutectic particles in contact with a germanium film are also present in the images apart from the eutectic particles that are present on the carbon sublayer and make the main contribution to the detected effects (Fig. 7). If the eutectic is considered to wet germanium, the temperature  $\approx 310^\circ\text{C}$  corresponds to the solidification of a liquid Au–Ge phase in contact with germanium.

### CONCLUSIONS

The use of a quartz resonator was shown to be effective for detecting the melting–solidification phase transformations in nanofilm systems with various characters of coupling forces and types of conduction. The melting–solidification temperature hysteresis in the Bi/C system was analyzed, and the detected phase-transition temperatures were shown to correspond to the data obtained by other methods. The supercooling during the solidification of the Ge–Au eutectic on an amorphous carbon substrate was found to be 165 K.

### ACKNOWLEDGMENTS

This work was supported by the Ministry of Education and Science of Ukraine (project no. 0109U001331).

### REFERENCES

1. O. S. Mei and K. Lu, *Prog. Mater. Sci.* **52**, 1175 (2007).
2. *Surface Phenomena and Phase Transformation in Condensed Films*, Ed. by N. T. Gladkikh (KhNU im. V. N. Karazina, Khar'kov, 2004) [in Russian].
3. M. Mitome, *Surf. Sci.* **442**, 953 (1999).
4. S. I. Bogatyrenko, A. V. Voznyi, N. T. Gladkikh, and A. P. Kryshstal, *Phys. Met. Metallogr.* **97**, 273 (2004).
5. M. M. Kolendovskii, S. I. Bogatyrenko, A. P. Kryshstal<sup>2</sup>, S. V. Dukarov, N. T. Gladkikh, and R. V. Sukhov, *Adgeziya Rasplavov Paiki Mater.* **40**, 40 (2007).
6. M. Zang, M. Yu. Efremov, F. Schiettekatte, et al., *Phys. Rev. B* **62**, 10549 (2000).
7. J. Freden, *Handbook of Modern Sensors: Physics, Designs and Applications* (Springer, San Diego, 2004).
8. G. Sauerbrey, *Z. Phys.* **155**, 206 (1959).
9. K. K. Kanazawa and J. G. Gordon, *Anal. Chem.* **57**, 1770 (1985).
10. C. Sang-Mok, K. Jong-Min, H. Muramatsu, T. Ataka, C. WonJei, and H. I. Chang-Sik, *Polymer* **37**, 3757 (1996).
11. F. J. B. Kremera, H. Ringsdorf, A. Schuster, M. Seitz, and R. Weberskircha, *Thin Solid Films* **284–285**, 436 (1996).
12. M. Rodahl and B. Kasemo, *Sens. Actuators A* **54**, 448 (1996).
13. H. Okamoto, *Phase Diagrams for Binary Alloys* (ASM International, 2000).
14. L. N. Chepurnaya, A. P. Kryshstal<sup>2</sup>, S. I. Bogatyrenko, M. M. Kolendovskii, and N. T. Gladkikh, *Fiz. Inzh. Poverkhn.* **5**, 79 (2007).
15. A. P. Kryshstal, N. T. Gladkikh, and Sukhov, *Appl. Phys. Sci.* **257**, 338 (2011).
16. *Piezoelectric Sensors*, Ed. by A. Langhoff and C. Steinem (Springer, 2007), Vol. 5.
17. M. Urbakh and L. I. Daikhin, *Colloid. Surf. A* **134**, 75 (1998).
18. N. T. Gladkikh, A. P. Kryshstal<sup>2</sup>, and R. V. Sukhov, *Nanosist. Nanomater. Nanotekhnol.* **8**, 79 (2010).

*Translated by K. Shakhlevich*

### SPELL OK